International Journal of Electrical, Electronic and Communication Sciences
ISSN: 2517-9438
Vol:11, No:3, 2017

All-Silicon Raman Laser with Quasi-Phase-Matched Structures and Resonators

Isao Tomita

Abstract—The principle of all-silicon Raman lasers for an output wavelength of 1.3 μm is presented, which employs quasi-phase-matched structures and resonators to enhance the output power. 1.3-μm laser beams for GE-PONs in FTTH systems generated from a silicon device are very important because such a silicon device can be monolithically integrated with the silicon planar lightwave circuits (Si PLCs) used in the GE-PONs. This reduces the device fabrication processes and time and also optical losses at the junctions between optical waveguides of the Si PLCs and Si laser devices when compared with 1.3-μm III-V semiconductor lasers set on the Si PLCs employed at present. We show that the quasi-phase-matched Si Raman laser with resonators can produce about 174 times larger laser power at 1.3 μm (at maximum) than that without resonators for a Si waveguide of Raman gain 20 cm/GW and optical loss 1.2 dB/cm, pumped at power 10 mW, where the length of the waveguide is 3 mm and its cross-section is (1.5 μm)^2.

Keywords—All-silicon raman laser, FTTH, GE-PON, quasi-phase-matched structure, resonator.

I. Introduction

At present, 1.31-μm III-V semiconductor laser diodes are being used as signal transmitters at the end-user side of the Gigabit Ethernet-Passive Optical Network (GE-PON) in the Fiber-To-The-Home (FTTH) systems [1], [2]. Here, these III-V laser diodes are hybridly integrated with silicon planar lightwave circuits (Si PLCs) in the GE-PON. In order to reduce the number of the fabrication processes and thus the fabrication time of the signal transmitters, the development of Si light sources is indispensable so that they can be monolithically integrated with the Si PLCs. The benefit of this monolithic integration is that it can reduce optical losses at the junction between optical waveguides of the Si PLCs and Si light sources.

Unfortunately, Si in the bulk, classified as indirect bandgap semiconductors, cannot emit light even if inverted population is formed. For this reason, light emission or laser-beam generation from Si has been performed by use of amplified spontaneous emission in low-dimensional structures [3], [4] or amplified stimulated Raman scattering (SRS) [5], [6], respectively, where both methods utilize resonators. But the output wavelengths obtained in these methods were $\sim$ 0.7-1.0 μm [3], [4] or $\sim$ 1.67-1.69 μm [5], [6], respectively, and thus cannot be used for the 1.31-μm signal transmitters.

In this paper, we present a method for generating 1.3-μm laser beams from a Si waveguide with SRS for the anti-Stokes waves. This is different from the ordinary SRS for the generation of the Stokes waves with a longer wavelength ($\sim$ 1.67-1.69 μm) than the pump-beam wavelength ($\sim$ 1.55 μm) [5], [6] due to frequency down-conversion. It is known that anti-Stokes waves, generated by frequency up-conversion, have a large optical phase mismatch for the anti-Stokes-wave generation unlike that for the Stokes-wave generation, thus giving a very small power to the growth of the anti-Stokes waves [7], [8]. To remove this phase mismatch, we employ a quasi-phase-matched structure in the Si waveguide and boost the output power. Here we should note that the anti-Stokes-wave generation requires the Stokes-wave generation [9]; Actually, the anti-Stokes-wave intensity $I_{\rm AS}$ is proportional to the Stokes-wave intensity $I_{\rm S}$ as $I_{\rm AS} \propto I_{\rm S} I_{\rm P}^2$, where $I_{\rm P}$ is the pump-beam intensity. To boost the anti-Stokes-wave power while decreasing the Stokes-wave power obtained *outside* the waveguide, we employ resonators that reflect the Stokes waves back to the waveguide and let the anti-Stokes waves pass through the resonators, as shown in Fig. 1, where the pump beam can also pass through the resonators.

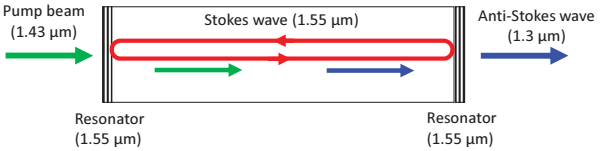

Fig. 1 Device principle

Such resonators can easily be fabricated with ordinary dielectric multilayer mirrors with an appropriate multilayer period. In the next section, we show the analysis of the output characteristics in the quasi-phase-matched Si Raman laser using the anti-Stokes-wave generation with such resonators.

II. Analysis Method for Output Characteristics

We depict our device model for the output-characteristic analysis in Fig. 2.

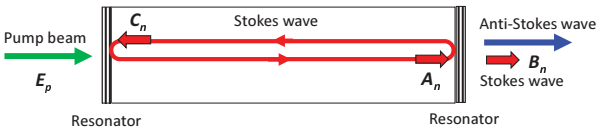

Fig. 2 Device calculation model

In Fig. 2, resonators made of dielectric multilayer mirrors with a reflection amplitude of r and a transmission amplitude of t (r and t are real numbers) are set at the both sides of the device with a length of L, where only the Stokes

Isao Tomita is with Department of Electrical and Computer Engineering, National Institute of Technology, Gifu College, 2236-2 Kamimakuwa, Motosu, Gifu 501-0495, Japan (e-mail: itomita@gifu-nct.ac.jp).

waves, generated inside the device from a pump beam, are reflected with resonators having a proper multilayer period. In this device, we use a quasi-phase-matched waveguide, or $\chi^{(3)}$-periodic waveguide, as shown in Fig 3, where the phase mismatch for the anti-Stokes waves is removed by taking an appropriate quasi-phase-matching period Λ. As will be shown later, we employ $\Delta\chi^{(3)}$ as a difference between the maximum and minimum sizes of $\chi^{(3)}$ in the waveguide (No quasi-phase matching occurs if $\Delta\chi^{(3)} = 0$).

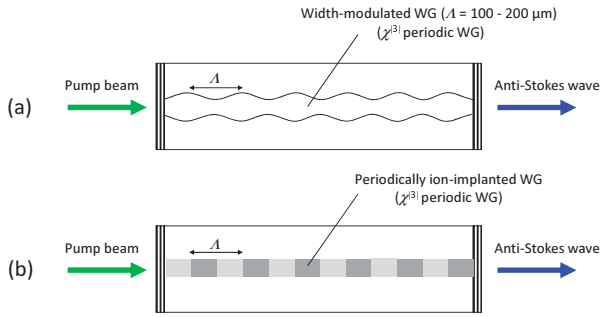

Fig. 3 (a) Device with a $\chi^{(3)}$-periodic structure made of a width-modulated waveguide, (b) Device with a $\chi^{(3)}$-periodic structure made of a periodically ion-implanted waveguide

In Fig. 2, we set λ as the Stokes wavelength, $E_{\rm p}$ as the pump-electric-field amplitude, θ as the phase shift of the waves at reflection with the resonators. We then have the following recurrence relations for the electric-field amplitudes A_n, B_n, C_n $(n > 1)$:

$$A_n = E_{\rm p}\, e^{(g-\alpha)\frac{L}{2}} e^{i2\pi\frac{L}{\lambda}} + re^{i\theta} C_{n-1}\, e^{(g-\alpha)\frac{L}{2}} e^{i2\pi\frac{L}{\lambda}}, \quad (1)$$

$$B_n = t\, A_n, \quad (2)$$

$$C_n = re^{i\theta} A_n\, e^{(g-\alpha)\frac{L}{2}} e^{i2\pi\frac{L}{\lambda}}, \quad (3)$$

where A_n is the amplitude of the right-going Stokes waves inside the device, B_n is that of the Stokes waves going outside the device, C_n is that of the left-going Stokes waves inside the device, n represents the circulation number, g is set as $g = G|E_{\rm p}|^2$ ($|E_{\rm p}|^2$ = constant is assumed) with a Si Raman gain of G, and α is the beam propagation loss.

For the first Stokes-wave generation inside the device (i.e., $n = 1$), A_n, B_n, and C_n must satisfy

$$A_1 = E_{\rm p}\, e^{(g-\alpha)\frac{L}{2}} e^{i2\pi\frac{L}{\lambda}}, \quad (4)$$

$$B_1 = t\, A_1, \quad (5)$$

$$C_1 = re^{i\theta} A_1\, e^{(g-\alpha)\frac{L}{2}} e^{i2\pi\frac{L}{\lambda}}. \quad (6)$$

By solving the recurrence relations (1)-(3) with the initial conditions (4)-(6) taken into account, we obtain

$$|E_{\rm S}|^2_{\rm in} \equiv |A_\infty|^2 = \beta |E_{\rm p}|^2 e^{(g-\alpha)L}, \quad (7)$$

$$\beta = \frac{1}{1 - 2r^2 e^{(g-\alpha)L}\cos\delta + r^4 e^{2(g-\alpha)L}}, \quad (8)$$

$$\delta = 2\theta + 4\pi\frac{L}{\lambda}, \quad (9)$$

where an infinite recurrence number $(n \to \infty)$ has been taken with an assumption of $r^2 e^{(g-\alpha)L} < 1$ [10], $\beta\,(> 1)$ is the intensity enhancement factor for the Stokes waves inside the device ($\beta = 1$ corresponds to the non-resonator case), δ is a phase shift, and $|E_{\rm S}|^2_{\rm in}$ denotes the Stokes-wave intensity inside the device. The Stokes-wave intensity outside the device, denoted by $|E_{\rm S}|^2_{\rm out}$, is calculated as

$$|E_{\rm S}|^2_{\rm out} \equiv |B_\infty|^2 = \gamma |E_{\rm p}|^2 e^{(g-\alpha)L}, \quad (10)$$

$$\gamma = (1 - r^2)\beta, \quad (11)$$

where γ is the intensity enhancement factor for the Stokes waves going outside the device. Furthermore, the anti-Stokes-wave intensity $|E_{\rm AS}|^2_{\rm out}$ going outside the device is calculated as

$$|E_{\rm AS}|^2_{\rm out} \approx (\Delta\chi^{(2)}/\chi^{(2)})^2\, G^2 |E_{\rm p}|^4 |E_{\rm S}|^2_{\rm in} L^2. \quad (12)$$

This shows that the intensity enhancement of the output anti-Stokes waves requires that of *the Stokes waves inside the device*, which is easily achieved with the resonators for the Stokes waves. As for the unit of $|E_{\rm i}|^2$ (i = P, S, AS), it is W/m^2 if we use the Raman gain G in units of m/W. To convert it to the unit W of a power P, we need to multiply it by the beam cross-section S, i.e., $P_{\rm i} = S|E_{\rm i}|^2$ (i = P, S, AS), which will be used to show numerical results in the next section.

III. Results

First, we show the resonator reflectance r^2 dependence of the intensity enhancement factors β and γ for the Stokes waves inside and outside the device in Figs. 4 and 5, respectively. Here we have employed a Si Raman gain of $G = 20$ cm/GW [11], a loss factor of $\alpha = 0.28$/cm (1.2 dB/cm) [12], a waveguide length of $L = 3$ mm, a waveguide cross-section of $S = (1.5\ \mu{\rm m})^2$, a pump-beam power of $P_{\rm p} = 10$ mW, and a $\chi^{(3)}$-difference of $\Delta\chi^{(3)}/\chi^{(3)} = 0.3$. These parameters satisfy the condition $r^2 e^{(g-\alpha)L} < 1$ for $0 \le r^2 \le 1$, where $g = G|E_{\rm p}|^2 = GP_{\rm p}/S$. The pump, Stokes, and anti-Stokes wavelengths are set to be $\lambda_{\rm P} = 1.43\ \mu$m, $\lambda_{\rm S} = 1.55\ \mu$m, $\lambda_{\rm AS} = 1.3\ \mu$m, respectively. In addition, the phase shift δ is set to be $2\pi m$ (m is an integer) by refractive-index adjustment of the device using temperature control.

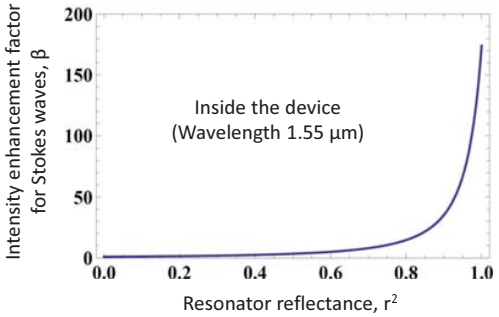

Fig. 4 Resonator reflectance r^2 dependence of the intensity enhancement factor β for the Stokes waves inside the device

From Fig. 4, we can see that β becomes large as r^2 increases because of the steady accumulation of Stokes-wave photons with the resonators and that β is about 174 at $r^2 = 1$, which means that the Stokes-wave power at $r^2 = 1$ is about 174

times larger than that without the resonators (i.e., at $r^2 = 0$). Fig. 5 shows that γ increases as r^2 approaches 0.92 from 0 and decreases rapidly if r^2 exceeds 0.92. At $r^2 = 1$, since $\gamma = 0$, no Stokes waves come outside the device.

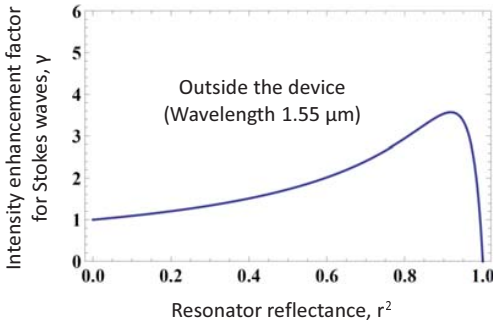

Fig. 5 Resonator reflectance r^2 dependence of the intensity enhancement factor γ for the Stokes waves outside the device

Next, in Fig. 6, we depict the resonator-reflectance r^2 dependence of the anti-Stokes power $P_{\rm AS}$ outside the device calculated from (12) with $P_{\rm AS} = S|E_{\rm AS}|^2$. $P_{\rm AS}$ becomes large as r^2 increases, which follows the feature of the Stokes-power enhancement inside the device. At $r^2 = 1$, we can obtain $P_{\rm AS} \approx 1.0$ μW, but when there are no resonators (i.e., $r^2 = 0$), $P_{\rm AS}$ is only 5.9 nW [13]. Additionally, in order to enhance the anti-Stokes power, a decrease in the cross-section of the waveguide is an effective way in addition to setting $r^2 = 1$.

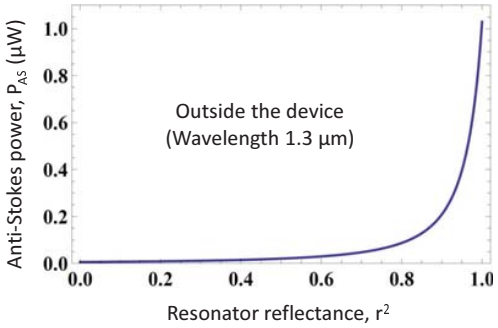

Fig. 6 Resonator-reflectance r^2 dependence of the anti-Stokes power $P_{\rm AS}$

In the next section, we describe how to fabricate the device with a $\chi^{(3)}$-periodic structure and resonators.

IV. Device Fabrication Method

It is possible to fabricate a $\chi^{(3)}$-periodic structure by use of a width-modulated waveguide, as shown in Fig. 3 (a). Actually, this type of waveguide has been used to enhance the output power in four-wave mixing [14]. In this structure, the optical intensity has a large value at the necks where the cross-section is small, and thus the effective $\chi^{(3)}$ has a large value there. In this way, a $\chi^{(3)}$ periodic structure can be obtained.

Detailed device fabrication processes containing that structure are shown in Figs. 7(a)-(e).

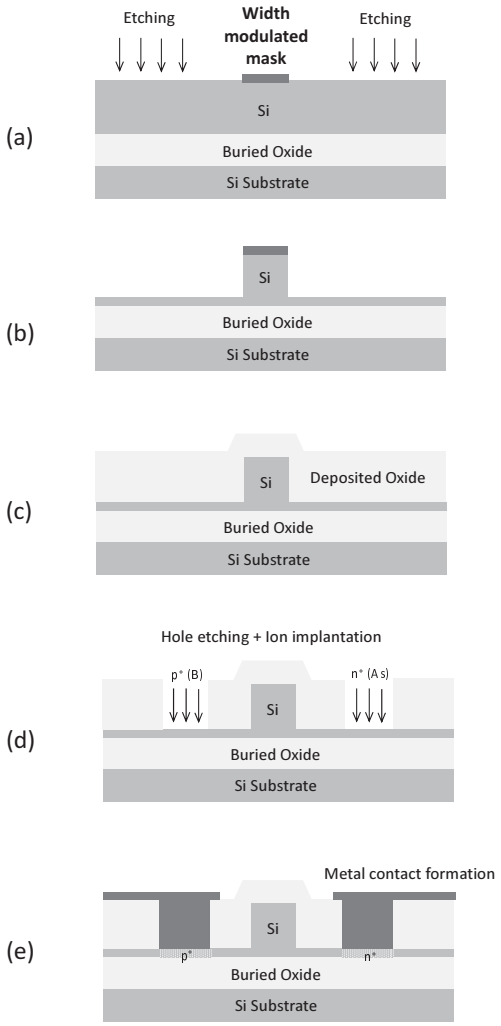

Fig. 7 Fabrication processes (a)-(e) for producing the device with a width-modulated waveguide

Using a width-modulated mask placed on a Si-on-insulator (SOI) wafer (Fig. 7 (a)), we etch the upper Si layer and form a width-modulated Si waveguide (Fig. 7 (b)).

Next, we fabricate a pn junction in the device, where a reverse bias is applied to remove created carriers when there is two-photon absorption. Unfortunately, even the longest 1.55-μm Stokes waves (with an energy of 0.8 eV) among the pump, Stokes, and anti-Stokes waves can excite carriers via two-photon absorption because of 2×0.8 eV = 1.6 eV $>$ 1.1 eV (1.1 eV is the Si bandgap energy). Thus the reverse-biased pn junction is necessary to decrease the optical loss caused by the excited free carriers.

To produce the pn junction, the deposition of oxides is performed on the etched surface after the removal of the upper mask (Fig. 7 (c)). After the creation of openings, or holes, at the oxide layer via etching, ion implantation is made through the holes by use of B for p-type Si and As for n-type Si (Fig. 7 (d)). After this ion implantation, metal contacts are formed through the holes (Fig. 7 (e)). At the final

procedure, we form dielectric multilayers on the front and back facets by deposition of layered dielectrics so that the device has resonators. In place of these dielectric multilayers, it is possible to use Bragg-grating reflectors, which are fabricated at both ends of the waveguide. In this case, the grating should be fabricated between the processes of Figs. 7 (b) and (c).

Another method to fabricate a $\chi^{(3)}$-periodic structure is to use spatially-periodic ion implantation on the upper Si layer of an SOI wafer. Since ion implantation randomizes the crystal-lattice structure, the size of $\chi^{(3)}$ will be reduced. By this method, as shown in Fig. 8 (a), we can create a $\chi^{(3)}$-periodic structure.

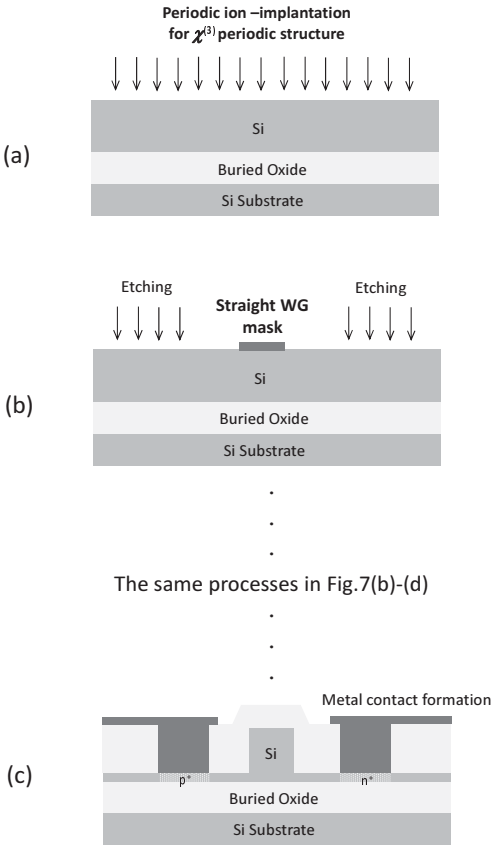

Fig. 8 Fabrication procedures (a)-(c) for producing the device with a spatio-periodically ion-implanted waveguide

To fabricate a waveguide, we set a straight mask on the spatio-periodically ion-implanted Si layer, and then etch the unmasked part (Fig. 8 (b)). After performing the same procedures, as given in Figs. 7 (b)-(d), we can fabricate a pn junction (Fig. 8 (c)). For resonators that should be placed at both ends of the waveguide, we use multilayer dielectrics or Bragg-grating reflectors, such as those mentioned above.

V. Summary

We have presented the principle of a quasi-phase-matched Si Raman laser with resonators to enhance 1.3-μm anti-Stokes waves that can be used for the signal transmitters in the GE-PONs of FTTH systems. Here we have removed the phase mismatch in the anti-Stokes waves using a $\chi^{(3)}$-periodic structure. Since the anti-Stokes-wave power is proportional to the Stokes-wave power, we have enhanced the Stokes-wave power with resonators that reflect the Stokes waves to accumulate them inside the device and let the anti-Stokes waves pass toward outside of the device. By this mechanism, we have obtained about 174 times larger laser power (at maximum) at 1.3 μm than that without resonators. Furthermore, we have shown the fabrication methods for such a device by use of a width-modulated waveguide or a spatio-periodically ion-implanted waveguide, which includes a free-carrier-loss decreasing mechanism with a pn junction.

Acknowledgment

The author would like to thank National Institute of Technology, Gifu College, for financial support.

References

[1] M. Iwase *et al.*, "Optical Transceiver Modules for Gigabit Ethernet PON FTTH System," Furukawa Rev. 28, 2005, pp. 8-14.
[2] H. Kanamori, "Passive Optical Components and Their Applications to FTTH Networks," SEI Tech. Rev. 73, 2011, pp. 14-21.
[3] S. Saito *et al.*, "Stimulated emission of near-infrared radiation by current injection into silicon (100) quantum well," Appl. Phys. Lett., 95, 2009, pp. 1101-1103.
[4] S. Saito *et al.*, "Stimulated emission of near-infrared radiation in silicon fin light-emitting diode," Appl. Phys. Lett. 98, 2011, pp. 1104-1106.
[5] H. Rong *et al.*, "An all-silicon Raman laser," Nature 433, 2005, pp. 292-294.
[6] H. Rong *et al.*, "A continuous-wave Raman silicon laser," Nature 433, 2005, pp. 725-727.
[7] R. Claps *et al.*, "Anti-Stokes Raman conversion in silicon waveguides," Opt. Exp. 11, 2003, pp. 2862-2872.
[8] O. Boyraz *et al.*, "Observation of simultaneous Stokes and anti-Stokes emission in a silicon Raman laser," IEICE Elec. Exp. 1, 2004, pp. 435-441.
[9] R. W. Boyd, Nonlinear Optics, 1st ed. (Academic Press, San Diego, 1992).
[10] N. Hodgson and H. Weber, Laser Resonators and Beam Propagation -Fundamentals, Advanced Concepts and Applications, 2nd ed. (Springer, Berlin, 2005). In our model, true lasing occurs when $r^2 e^{(g-\alpha)L} > 1$, but this gives rise to an infinitely large $|A_\infty|^2$, particularly at $r^2 = 1$. This would melt the device, and was avoided in our paper.
[11] R. Claps *et al.*, "Observation of stimulated Raman amplification in silicon waveguides," Opt. Exp. 11, 2003, pp. 1731-1739.
[12] K. K. Lee, D. R. Lim, L. C. Kimerling, J. Shin, and F. Cerri, "Fabrication of ultralow-loss Si/SiO_2 waveguides by roughness reduction," Opt. Lett. **26**, 2001, pp. 1888-1890. Since this paper reported 0.8 dB/cm as an optical loss of a Si waveguide, the fabrication of a waveguide with a loss of 1.2 dB/cm in our paper is possible.
[13] E. Hecht, Optics, 4th ed. (Pearson Education, Essex, 2002). In our model, the reflection of the anti-Stokes waves at the interface between the Si waveguide and the outside air is ignored. Only Stokes waves are reflected with the resonators. But actually, about 30% of the anti-Stokes waves are reflected at the interface even when there are no resonators, so that actually obtainable $P_{\rm AS}$ is about $0.7\,P_{\rm AS}$.
[14] J. B. Driscoll *et al.*, "Width-modulation of Si photonic wires for quasi-phase-matching of four-wave-mixing: experimental and theoretical demonstration," Opt. Exp. 20, 2012, pp. 9227-9242.